

Some considerations on the water polymorphism and the liquid-liquid transition by the density behavior in the liquid phase

Cite as: *J. Chem. Phys.* **151**, 044504 (2019); <https://doi.org/10.1063/1.5095687>

Submitted: 12 March 2019 . Accepted: 01 July 2019 . Published Online: 29 July 2019

Francesco Mallamace , Carmelo Corsaro , Domenico Mallamace , Enza Fazio , and Sow-Hsin Chen

COLLECTIONS

Paper published as part of the special topic on [Chemical Physics of Supercooled Water](#)

Note: This paper is part of a JCP Special Topic on Chemical Physics of Supercooled Water.



[View Online](#)



[Export Citation](#)



[CrossMark](#)

ARTICLES YOU MAY BE INTERESTED IN

[On the link between polyamorphism and liquid-liquid transition: The case of salty water](#)
The Journal of Chemical Physics **151**, 044503 (2019); <https://doi.org/10.1063/1.5100959>

[Radial distribution functions of water: Models vs experiments](#)
The Journal of Chemical Physics **151**, 044502 (2019); <https://doi.org/10.1063/1.5100871>

[Is water one liquid or two?](#)
The Journal of Chemical Physics **150**, 234503 (2019); <https://doi.org/10.1063/1.5096460>

Lock-in Amplifiers
up to 600 MHz



Some considerations on the water polymorphism and the liquid-liquid transition by the density behavior in the liquid phase

Cite as: *J. Chem. Phys.* **151**, 044504 (2019); doi: 10.1063/1.5095687

Submitted: 12 March 2019 • Accepted: 1 July 2019 •

Published Online: 29 July 2019



View Online



Export Citation



CrossMark

Francesco Mallamace,^{1,2,a)} Carmelo Corsaro,³ Domenico Mallamace,³ Enza Fazio,³ and Sow-Hsin Chen¹

AFFILIATIONS

¹ Department of Nuclear Science and Engineering, Massachusetts Institute of Technology, Cambridge, Massachusetts 02139, USA

² Istituto dei Sistemi Complessi, Consiglio Nazionale delle Ricerche, 00185 Roma, Italy

³ Dipartimento di Scienze Matematiche e Informatiche, Scienze Fisiche e Scienze della Terra (MIFT), Università di Messina I-98166, Messina, Italy

Note: This paper is part of a JCP Special Topic on Chemical Physics of Supercooled Water.

^{a)} Electronic mail: francesco.mallamace@unime.it

ABSTRACT

The bulk liquid water density data (ρ) are studied in a very large temperature pressure range including also the glass phases. A thorough analysis of their isobars, together with the suggestions of recent thermodynamical studies, gives evidence of two crossovers at T^* and P^* above which the hydrogen bond interaction is unable to arrange the tetrahedral network that is at the basis of the liquid polymorphism giving rise to the low density liquid (LDL). The curvatures of these isobars, as a function of T , are completely different: concave below P^* (where maxima are) and convex above. In both the cases, a continuity between liquid and glass is observed with P^* as the border of the density evolution toward the two different polymorphic glasses (low and high density amorphous). The experimental data of the densities of these two glasses also show a markedly different pressure dependence. Here, on the basis of these observations in bulk water and by considering a recent study on the growth of the LDL phase, by decreasing temperature, we discuss the water liquid-liquid transition and evaluate the isothermal compressibility inside the deep supercooled regime. Such a quantity shows an additional maximum that is pressure dependent that under ambient conditions agrees with a recent X-ray experiment. In particular, the present analysis suggests the presence of a liquid-liquid critical point located at about 180 MPa and 197 K.

Published under license by AIP Publishing. <https://doi.org/10.1063/1.5095687>

I. INTRODUCTION

Water and related systems have a central role in science and technology. At the same time, water is of absolute interest in many research fields going from chemical-physics to life sciences such as medicine, biology crossing agriculture, and engineering.¹ It has unusual behaviors, if compared with normal liquids. The first and well known example of these is the density maximum (ρ_M at 277 K) intuited by Galileo Galilei in 1612² and later discovered by Florence.³ Many of these anomalies belong to water in the metastable supercooled state and characterize the thermodynamical behaviors of important response functions, e.g., the isobaric

specific heat ($C_P = T(\partial S/\partial T)_P$), the compressibilities {isothermal [$\kappa_T = (\partial \ln \rho / \partial \ln P)_T$] and adiabatic [$\kappa_S = (\partial \ln \rho / \partial \ln P)_S$]}, and the expansivity ($\alpha_P = -(\partial \ln \rho / \partial T)_P$). All these functions are associated with the system microscopic fluctuations, more precisely: κ_T with the volume V or density ($\kappa_T = \langle (\delta V)^2 \rangle / k_B T V$), C_P with the entropy S ($C_P = \langle (\delta S)^2 \rangle / k_B T$), whereas α_P reflects the volume-entropy cross correlations ($\alpha_P = \langle \delta S \delta V \rangle / k_B T V$). Water can be cooled below its melting temperature (T_m) up to the homogeneous nucleation temperature (T_h), and both are pressure dependent.

The behaviors of these fluctuations give rise to two important observations.⁴ The first one is regarding the δS and δV difference on

cooling between a normal liquid and water; in a normal fluid, both these fluctuations become smaller as T decreases; on the contrary, in water, they become more pronounced; in most of the normal liquids, they are positively correlated (an increase in δV is accompanied by a similar behavior in δS); instead for water, below T_m , they are anticorrelated (an increase in V brings an entropy decrease). Thus, the water cooling is accompanied by an increase in its local order, and these anticorrelations become increasingly pronounced for water inside the supercooled state. In addition to this, another salient water property, easily observed at ambient pressure, is that its thermodynamic response functions show, as observed for the first time by Speedy and Angell,⁵ a diverging (critical) behavior; extrapolated from their measured values at moderate supercooling to the lowest temperatures, all these functions appear to diverge at a singular temperature $T_S \sim 228$ K.

As it is well known, these results were lately related to the liquid polymorphism possibility of a first-order phase transition between two liquids of the same substance.⁶ The possibility of two liquids of the same substance was proposed by Rapoport in 1967⁷ by considering several studies on the continuous change in the liquid water state over the wide P-T region,⁸⁻¹¹ based on the idea of multiple species coexisting in the liquid. However, only after the Mishima evidence for the existence of the multiple distinct amorphous phases (1985), the liquid-liquid transition (LLT) hypothesis becomes central in the water studies.⁶

The Speedy and Angell observations coming from the response functions, i.e., the entropy decrease and the diverging behavior, can be considered at the basis of the water complexity and of the enormous interest in it. Nowadays, whereas we are sure of the existence of a water molecular local order, with a tetrahedral symmetry driven by the hydrogen bonding (HB) interaction, the corresponding criticality (inside the supercooled regime) is far from being experimentally proven. This despite the incredible large number of computational studies made in the years, with their positive and proper suggestions.¹²

The HB is a noncovalent attractive interaction between two water molecules, i.e., an electropositive hydrogen atom on one molecule and an electronegative oxygen atom on another molecule [i.e., the O:H noncovalent van der Waals bond (≈ 0.1 eV binding energy BE)]. In contrast to the HB, there is in water also a repulsive intermolecular interaction: the Coulomb repulsion between electron lone-pairs on adjacent oxygen atoms. In addition, there are the two H-O covalent bonds originated by the sharing of the electron lone pairs, ≈ 4.0 eV. Whereas the HB dominates water in the stable and supercooled regime, the repulsive lone pairs mainly influence the water physics from above the boiling temperature (T_b) in the sub-critical and critical region (the water critical point CP is located at $T_C = 647.1$ K and $P_C = 22.064$ MPa).

The tetrahedral symmetry is that of ordinary ice, in which each water molecule has four nearest neighbors and acts as a H-donor to two of them and a H-acceptor for the other two. Whereas ice is a permanent tetrahedral network made by the HB, the liquid water tetrahedrality is local and transient even if characterized by a lifetime that strongly increases (more than three orders of magnitude) by decreasing temperature from values of some picoseconds characteristic of the stable liquid phase ($T > T_m$).¹³ All of this takes place in coherence with the response function behaviors on cooling, the entropy increases (because $C_P > 0$) as well as the specific volume

($V_S = 1/\rho$), due to the progressive increase in the tetrahedral order. In such a way, at ambient pressure, δV and δS can become anti-correlated and $\alpha_P < 0$. However, a pressure increase contrasts these ordering effects imposing different thermodynamical behaviors so that proper observations on increasing P certainly can give information on the water open questions including its criticality in the supercooled regime.

Like the structure, also the dynamic or transport water properties are unusual. When water is sufficiently cold, its diffusivity increases with pressure, whereas its viscosity decreases; this is due to the P -effect that tends to deform (or destroy) the tetrahedral HB network (and to change the internal structure of a single molecule), by increasing consequently the molecular mobility. The pressure behavior in connection with the HB water network, studied up to 400 MPa and temperatures near 200 K,^{13,14} by means of a NMR experiment, reveals that for each isotherm, the self-diffusion D_S increases with P to a maximum located near 200 MPa after which it decreases; on the contrary, the temperature behavior can be described with the same scaling law [$D_S(T) = D_0((T - T_S)/T_S)^{-\gamma}$] used by Speedy and Angell⁵ in their pioneering experiment in which a sort of water criticality in the supercooled regime was proposed. Such a study for the first time supports this latter conjecture in terms of transport parameters, but a careful inspection of the reported data for both H₂O and D₂O suggests that ~ 200 MPa (where each D_S isotherm has the maximum) is the limit of pressure deformation effects on the HB network, or the pressure value enough to change it completely. On the other hand, we must mention that just NMR experiments have revealed that there is a crossover temperature at $T^* \sim 315$ K for which by decreasing T liquid, water changes its energetic behavior from Arrhenius to super-Arrhenius.¹⁵ In particular, for $T^* < 315$ K, it is observed that the Stokes-Einstein relation adequately describes the relative temperature dependence of viscosity and diffusion, but above and in the vicinity of such a temperature, the spin lattice relaxation does not follow the viscosity as predicted by this law. Lately, by using the Adam-Gibbs approach, it has been demonstrated that such a temperature can be considered as the onset of the HB tetrahedral network.¹⁶

The knowledge about water characteristics has improved markedly after the discovery of its polyamorphism, i.e., the existence of glassy forms with different densities. Depending on P and T , water has two amorphous phases characterized by different structures: the high density and the low density amorphous, HDA and LDA, respectively.¹⁷⁻¹⁹ HDA can be formed by the LDA, and vice versa. At the ambient pressure, LDA if heated undergoes a glass to liquid transition (at about 130 K) into a highly viscous fluid and then, at $T_x = 150$ K, crystallizes into cubic ice. Hence, in the region between T_x and T_h , water cannot stably exist in its bulk liquid form. Such a constraint can be overcome by using some tricks: to confine water in nanopores (radius 1–2 nm) smaller than nucleation centers, to study water inside ice, and to melt a multimolecular thickness of ice surface. Although these tricks have allowed the discovery of many important water properties, such as the existence of a density minimum, as predicted more than a century ago by Bridgeman,²⁰ and to give proper models for the supercooled state,¹⁴ here we will not give special focus to these results. This is to avoid any possible sterile discussions about the difference between confined and bulk water.

The HDA glass is obtained, at low temperatures, by the pressure-induced amorphization of the bulk ice (I_h). At 77 K and $P \approx 1$ GPa, the HDA density is about 1.31 g cm^{-3} . If the HDA at ambient pressure is heated, a new transformation occurs at $\sim 117 \text{ K}$ ¹⁷; this new amorphous, the LDA, has a density of 0.94 g cm^{-3} at 77 K and $P \approx 0.1 \text{ MPa}$. HDA can be produced at 77 K by compressing ice I_h at $\approx 1 \text{ GPa}$ or by compressing, at the same temperature, LDA at $\approx 0.6 \text{ GPa}$. For $P > 0.8 \text{ GPa}$ and $T > 130 \text{ K}$, another amorphous phase named VHDA (very high density amorphous) has been obtained.²¹

The two mentioned water glasses have two different local arrangements; HDA has a structure very similar to that of the high- P liquid water, suggesting that, as confirmed by the measured densities in the P - T plane (see Fig. 2), it is the glass form of the high- P liquid water, just as LDA may be a glass form of the low- P liquid water. It must be mentioned at this point that careful experiments arranged by the Loerting team have proposed the existence of a first order transition between these water amorphous phases.²²⁻²⁴ More precisely, all these three amorphous water states are connected so that they can be obtained (with a discontinuous transition) along a single isothermal compression (and decompression) experiment with the reversible sequence $LDA \rightleftharpoons HDA \rightleftharpoons VHDA$. An example of this is the compression \rightleftharpoons decompression induced LDA-HDA transitions in the T -range 138–140 K. In this latter case, the cycling pressure is about 200 MPa. It must be also stressed that the LDA-HDA transition is discontinuous, and recently it has been shown that in the HDA-VHDA transition, there are continuous intermediate states.²⁴

As discussed above, the water polyamorphism and the relative transitions led to considering the idea of two distinct liquid

phases, characterized by different densities, coexisting in liquid water, namely, the low density (LDL) and the high density (HDL) liquids. Such an idea benefits by the following experimental assurances: (i) high- T bulk liquid water, if rapidly cooled at ambient pressure, becomes LDA without crystallization so that LDA appears directly related to the liquid and²⁵ (ii) the HDA is connected with the liquid at high P , by the melting of crystalline ice on increasing pressure (the two amorphous having small entropies can be considered smoothly connected with the liquid state). These facts and the observed amorphous transitions give increasing support to a liquid-liquid transition (LLT) and also the possibility of a first-order phase transition in the liquid. In 1992 by taking into consideration the discontinuous LDA-HDA transitions, and the findings of a MD simulation, Poole *et al.* stressed the large possibility that supercooled water is really polymorphic, with the two glass phases as their evolution at the dynamical arrest.⁶ In such a way, it has also opened a possible explanation on the anomalies in the water's response functions in the supercooled state by means of a liquid-liquid critical point (LLCP) (also named second critical point in distinction to the vapor-liquid one). For clarity, the same laboratory has proposed an alternative interpretation for the water anomalies independently of the polymorphism.²⁶ However, these works can be considered as a milestone because they brought the interest of the scientific community to the fascinating research subject, which to date is still an open question: does water have a second critical point? The LLCP also focuses the role of the so-called Widom line (WL), that is, the locus of the maximum correlation length; along this line, the response functions reach extremes and increase on approaching the critical point, where they diverge (the WL can also be considered an extension of the coexistence curve). Figure 1 proposes a water phase diagram made

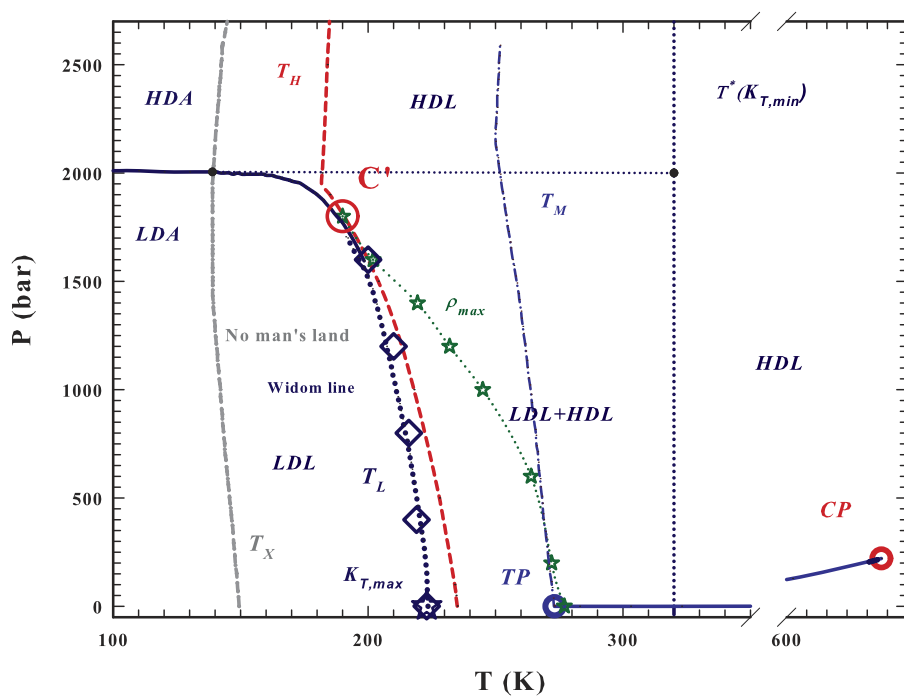


FIG. 1. The water phase diagram in the T - P plane. The following temperature lines are illustrated: the melting T_M , homogeneous nucleation T_H , density maxima ρ_{\max} , Widom line T_L , isothermal compressibility minimum T^* , and crossover from the liquid to the amorphous phase T_X . The critical point positions [the well-known liquid-gas CP and the proposed liquid-liquid C' (estimated value⁵)] and the triple point, TP , are also reported. Finally, the existence areas of the two amorphous phases LDA and HDA are proposed together with the regions characterized by the liquid polymorphism (LDL and HDL).

according to the LLCP hypothesis. Unfortunately, as it is well known, any exploration regarding bulk water seems to be forbidden in the region between T_x and T_h (called the no man's land) unless, as said, some tricks would be used, i.e., the water confinement²⁸ or some special techniques such as the recent pulsed-laser-heating one, which is able to determine the crystalline-ice growth rate and liquid-water diffusivity under ultrahigh-vacuum conditions (as made for temperatures between 180 and 262 K).²⁹

Our study is addressed just to the verification of this: is there in water a second critical point and is it dependent from the liquid polymorphism? We will explore such a question just on looking at the liquid water densities (or the specific volumes) in very large temperature and pressure regions, ranging from those of the vapor-liquid to the ones in the deep supercooled regime, also including the values corresponding to LDA and HDA. We have to mention that the structure and the densities of the HDL and LDL water have been measured by means of a neutron scattering experiment made at $T = 268$ K and at the pressures of 26, 209, and 400 MPa.²⁷

II. RESULTS AND DISCUSSIONS

The large number of studies made in confined water, by the use of very different experimental techniques ranging from the scattering (elastic and inelastic) to the calorimetry and including NMR, ESR, and FTIR spectroscopy, has given many results inside on what happens in the temperature region between T_x and T_h , such as a density minimum, the evidence of the LDL, the existence of the Widom line, a minimum with negative values in the expansivity α_p , a maximum in the specific heat C_p and in the isothermal compressibility κ_T , a dynamical crossover from fragile to strong glass-former behavior coincident with the Widom line, and the observation at this crossover of the violation of the Stokes-Einstein relation (with the consequent onset of the dynamical heterogeneities and the decoupling between the translational and rotational modes).²⁸ In this work, we will not mention these results and the related thermodynamics even if confined water for many aspects is more relevant than the bulk one. We will use some density data coming from MD simulations^{30-33,52} just for comparison with the results related to the minimum.^{34,35}

Figure 2 illustrates, in the top panel, the isobars of bulk water densities in the disordered states for a temperature interval from 70 to 700 K (i.e., from the values of the two amorphous phases LDA and HDA and the supercooled liquid state to the region of the liquid-vapor critical point); the pressures range from 0.1 to 800 MPa. The illustrated data come from different experiments arranged in the years in different laboratories; in particular, the figure reports data of LDA and HDA^{17,21,23,25} and bulk liquid water,^{20,36-42} and for the high temperature region, near the CP, data come from the 58-coefficient equation of state.⁴³ In the bottom panel of Fig. 2, the same data of the top panel with a low temperature zoom up to 350 K are reported, including also the data coming from a simulation of the equation of state by using the TIP4P/2005 water model³¹ and for water inside hydrophilic nanotubes.^{34,35} In this figure, the density values measured in ice Ih, Ic, and ice III (in such a case at the pressures of 260 and 350 MPa) are also reported;^{20,56} this is just for comparison with the water densities in the supercooled liquid state. From these data, there is direct

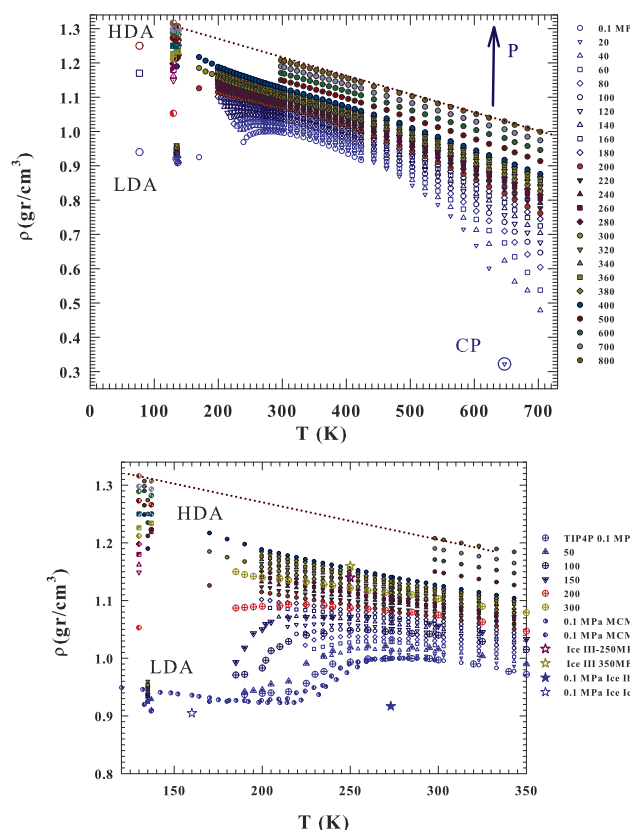


FIG. 2. Top—The bulk water density isobars, from 0.1 to 800 MPa, in the T range from 70 to 700 K (i.e., from the values of the two amorphous phases LDA and HDA to the region of the liquid-vapor critical point). The corresponding data come from some different experiments arranged in the years in different laboratories; in particular, the figure reports data of the LDA and HDA,^{17,21,23,25} and bulk liquid water,^{20,36-42} and for the high temperature region near C_P , data come from the 58-coefficient equation of state.⁴³ Bottom—The data are the same as illustrated above with a low temperature zoom up to 350 K. Are also included the densities coming from a simulation of the equation of state by using the TIP4P/2005 water model³¹ and of water inside hydrophilic nanotubes.^{34,35} The densities measured in ice Ih, Ic, and III are denoted as stars (in such a case for $P = 260$ and 350 MPa).^{20,56}

evidence on the density differences between liquid and crystalline water.

A careful inspection of the liquid water density data in the region where $T < 350$ K up to the amorphous phases evidences some interesting, important, and not negligible phenomena: (a) the density maximum, $\rho_{\max}(P, T)$, decreases with temperature by increasing its absolute value with P and disappears near 200 MPa; (b) the isobar curvature also changes by increasing P from concave to convex at about this pressure where $\rho_{\max}(P, T)$ disappears; (c) another important evidence that clearly comes out from the water density behavior is that 200 MPa is a crossover pressure between two well different $\rho(P, T)$ behaviors on cooling. For $P > 200$ MPa, the water densities evolve, with absolute continuity toward the values of the HDA (largely dependent on P in the range $1.15 < \rho < 1.33 \text{ g cm}^{-3}$, from 200 to 800 MPa), whereas for $P < 200$ MPa, the density evolution is

only toward the LDA, but contrary to the previous case, the P dependence of the LDA density ranges from 0.9 g cm^{-3} at 0.1 MPa to 0.93 g cm^{-3} at 200 MPa . Above this latter pressure, the melting curve in the P-T phase diagram changes its slope from negative to positive.

In any case, the $\rho(P, T)$ behavior illustrated by the figure indicates that the comparatively large density range, $0.93 < \rho < 1.15 \text{ g cm}^{-3}$, is barred for bulk water, not only at 135 K where we have the measured data of the amorphous phases but also, as confirmed by the curvature of the isobars, on going toward the region of the liquid phase (supercooled and stable). In other words, the isobars without the thermodynamical anomaly of the density maximum (minimum in the specific volume V_S) evolve with continuity to the corresponding HDA values. At the opposite side, the isobars that posses the maximum not only evolve toward the LDA density values (all located in the limited region of 0.9 – 0.93 g cm^{-3}) but can also have another anomaly like a minimum (maximum in V_S). This is the reason for which in the bottom panel of Fig. 2 we included density data coming from simulated and confined water. On considering that volume is a first derivative of the Gibbs free energy $G(T, P)$, $V = (\partial G / \partial P)_T$, such a situation is very interesting in the hypothesis of a LLCP; the fact that V_S has a marked discontinuity from 0.869 to $1.075 \text{ g}^{-1} \text{ cm}^3$, at $\sim 200 \text{ MPa}$, might represent a signature of a first-order phase transition.

We start our discussions on these bulk water density data (Fig. 2) from the main suggestion coming from the cited NMR dynamical data, for which the molecular mobility increases with P up to a maximum just at $\sim 200 \text{ MPa}$. This is due to the fact that pressure stresses the tetrahedral HB network. “Hence, one might consider hydrostatic pressure as a network breaking agent which suppresses long-range structural correlations.”¹³ A simple thermodynamical analysis of Fig. 2 density data fully confirms such a hypothesis. As said, the expansivity $\alpha_P = -(\partial \ln \rho / \partial T)_P = \langle \delta S \delta V \rangle / k_B T V$ represents a direct measure of the volume-entropy cross correlations. From these data, it clearly emerges that at all the isobars in which a density maximum $\rho_{\max}(T)$ is present for temperatures below it ($T < T_{\max}$), one has $\langle \delta S \delta V \rangle < 0$. Hence, for water in the liquid state, to a cooling process corresponds an entropy decrease, i.e., the order increases (the tetrahedral structure originated by the HB and its lifetime). Instead, for the isobars above $P^* \sim 200 \text{ MPa}$ at which the density maximum disappears and its curvature loses concavity ($P^* \sim 200 \text{ MPa}$, see Fig. 2), $\langle \delta S \delta V \rangle$ becomes positive together with the entropy giving proof of a structural disorder in the system. Such a situation is illustrated in Fig. 3 of Ref. 44.

At this point, just to avoid misunderstandings, it must be stressed that such a discussion on the pressures ability to destroy, or suppress, long-range HB structural correlations applies only to water in the metastable supercooled liquid state. Certainly, under stability conditions at the same T, P values, water is in the corresponding ice crystalline forms and the pressure effects on the system order are completely different.

The $\alpha_P(P, T)$ data highlight a special role for T^* ,^{16,44,45} from Fig. 2, it is also evident that such a temperature is that of the minimal density difference between all the reported isobars and of an ideal elasticity (the reported data change linearly with P). Such a situation can be better illustrated by plotting $\Delta\rho^* = \rho(T) - \rho(T^*)$, i.e., the difference between the densities measured at each isobar

with that measured at the corresponding T^* . The obtained result is illustrated in Fig. 3 for the range $120 < T < 375 \text{ K}$ (thus including the supercooled regime and the stable liquid phase). Certainly, for $T > 375 \text{ K}$, on approaching the subcritical and critical regions, where the dominating interaction is essentially the repulsion between electron lone-pairs, water dimers and trimers can also form. Instead, inside the stable liquid phase, the HB contribution increases on decreasing T and the local structure is made essentially by trimers and tetramers. As it can be observed, $\Delta\rho^*$ is pressure dependent for $T < T^*$ and also for $P \leq P^*$ (200 MPa). This is again an evidence of the presence of the HB tetrahedral network and of its response to external stresses (pressure or temperature). At the lowest pressures, $\Delta\rho^*$ presents the largest variation on cooling. By increasing pressure, such an effect progressively decreases. In addition, this local extended water structure is more sensitive to a temperature decrease in the pressure region where the density is maximum. Also here, the data deal only with bulk water, whereas the inset of Fig. 3 also reports the MD TIP4P/2005 and confined ones.^{31,34} These $\Delta\rho^*(T, P)$ data stress the two separate evolutions, on decreasing T , toward the arrest: liquid water merges in the LDA only if the applied pressure is $P < P^*$; otherwise, it gives rise to the HDA. Such a situation can be rationalized by considering the presence in the corresponding density isobars of the maximum indicating the increasing dominance on cooling of the LDL, made of HB tetrahedral networks, over the HDL; under such a condition, liquid water can glassify into the LDA. Instead in the opposite case, $P > P^*$, the applied pressure is enough to break, or to deform, the HBs, giving rise to the dominance of HDL over LDL so that because of the data continuity, water can evolve, on cooling, only into the HDA form. However, such a situation has the proper confirmation in the cited neutron scattering experiment on the existence of the HDL and LDL water liquid phases evaluating, at three different pressures, their relative population as x_{HDL} : for $P = 26 \text{ MPa}$, $x_{\text{HDL}} = 40\%$; for 209 MPa , $x_{\text{HDL}} = 60\%$; and for 400 MPa , $x_{\text{HDL}} = 80\%$.²⁷ All of this supports, in terms of the bulk water density, the liquid polymorphism and LLT hypothesis.

Figure 4, just to have further clarifications on the water thermodynamics, and to stress the previous findings especially in the supercooled regime, reports the corresponding P – V phase diagram ($V = V_S$). Also in this case, as illustrated in the inset, below P^* , it is clear that on decreasing T , the specific volume first decreases and then increases, whereas for $P > P^*$, only a continuous decrease in V_S can be observable. In particular, the data inside the supercooled regime will be treated taking in consideration the compelling evidence, coming from the physical conditions imposed by T^* and P^* , i.e., the LLCP could be located in the phase region $T < T^*$ and $P < P^*$. Next, we will use the reported data to evaluate the isothermal compressibility of bulk water in both the real critical point and the supercooled regime, where the LLCP may be located.

All the isotherms (continuous lines as a guide for the eyes) emphasize that in the supercooled region, an isotherm for which $(\partial^2 P / \partial V^2) = 0$ can be largely probable. The 273 K isotherm (dotted line) is the highest in which, at low pressures, a T decrease corresponds to a V_S decrease. Below it, any cooling imposes an increase in V_S that becomes progressively larger on going toward the supercooled regime, whereas in the high pressure region, V_S continues to keep the same decreasing rate. Thus, below 273 K , the inset of Fig. 4 gives a serious proof that the water isotherms are charac-

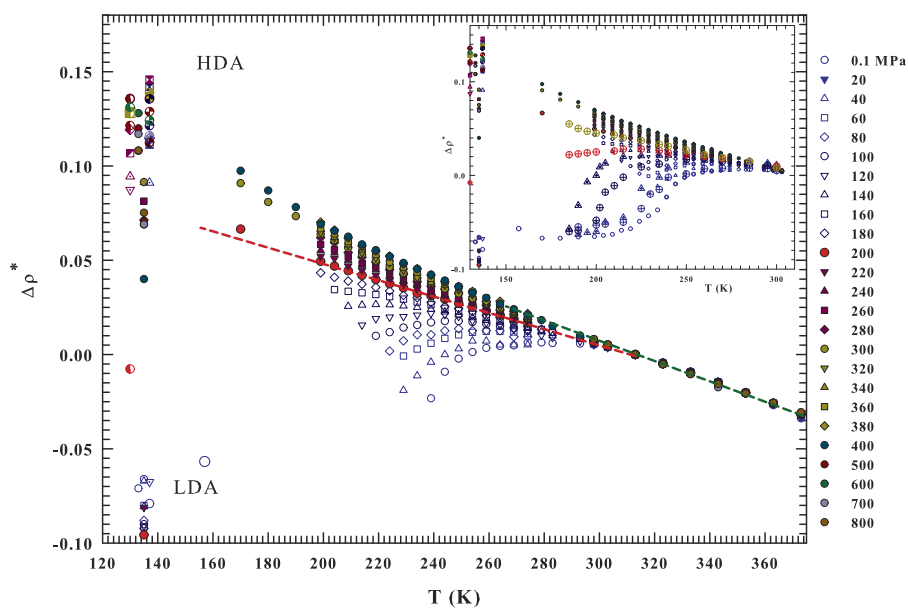


FIG. 3. The difference between each density isobar and that corresponding to T^* , i.e., $\Delta\rho^* = \rho(T) - \rho(T^*)$. The results are shown in the range $120 < T < 375$ K (including both the supercooled and the stable liquid phases). As it can be observed, $\Delta\rho^*$ is pressure dependent only for $T < T^*$, and also for $P \leq P^* = 200$ MPa. This is a compelling evidence of the presence of the HB tetrahedral network and its response to external stresses (pressure or temperature). At the lowest pressure, $\Delta\rho^*$ presents the largest variation on cooling, and by increasing pressure, such an effect progressively decreases. In addition, such a local extended water structure is more sensitive on cooling in the pressure region of the density maximum, i.e., $P < P^*$, if compared with the highest ones. The figure data deal only with bulk water, whereas in the inset, $\Delta\rho^*$ behaviors of the MD simulated TIP4P/2005 and confined ones are also reported.^{31,34}

terized by a progressive flattening on decreasing T and have a flex point. However, even if we do not have data in the no man's land, the reported isotherm behavior is fully consistent with the LLCP, in particular for the presence in the isotherms below 230 K of an

inflection point; among these, the critical one is that for which $(\partial^2 P / \partial V^2) = 0$.

Figure 5 reports the bulk water (and LDA) V_S , for some isobars in the intervals $170 < T < 320$ K and $0.1 < P < 300$ MPa;

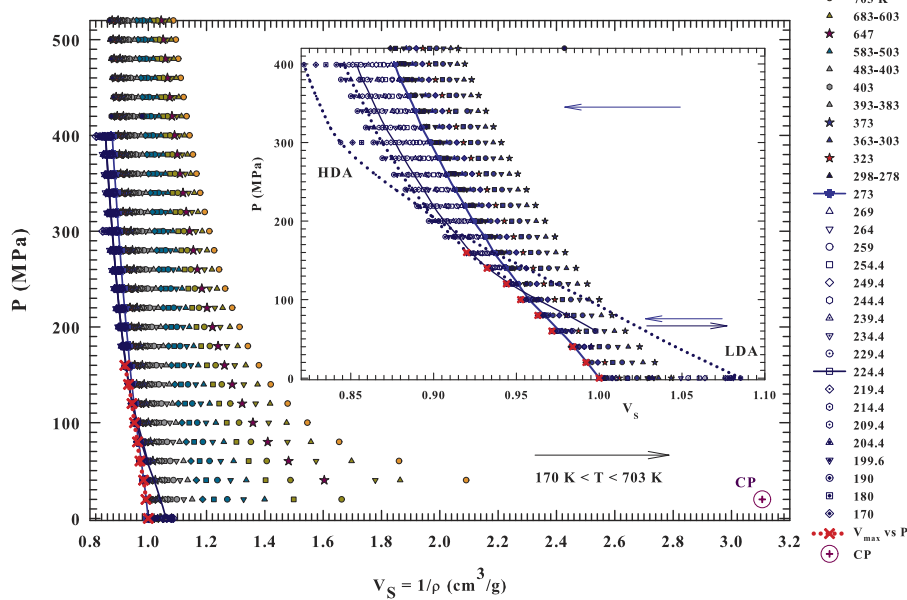


FIG. 4. The experimental P - V phase diagram. The specific volume ($V = V_S$) isotherms are proposed in a very large interval also including the critical region [with the critical point (CP) value]. As shown in the inset, it is evident that below P^* , on decreasing T , the specific volume first decreases and then increases, whereas for $P > P^*$, only a V_S continuous decrease can be observable. Such a singular data behavior gives again evidence that LLT, as far as the HB network, has extremes in the area delimited by T^* and P^* , i.e., the LLCP must be located in the phase region for $T < T^*$ and $P < P^*$.

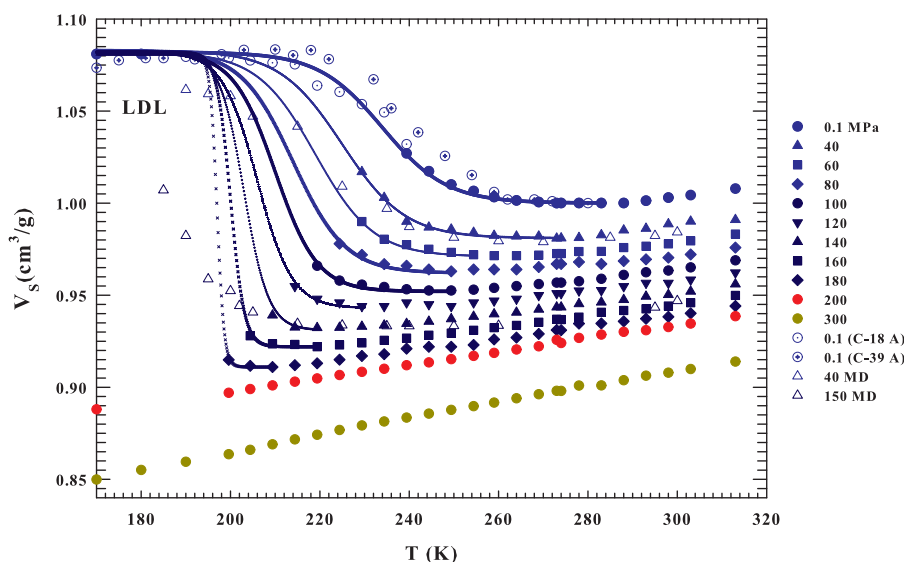


FIG. 5. The bulk water (and LDA) isobars of V_S measured inside the T -region $170 < T < 320$ K [the data for $P = 300$ MPa, which (open symbols) corresponding to the cited MD simulation (TIP4P/2005 model)³¹ and confined water^{34,35} are included]. The curves correspond to a data fit in terms of the same logistic function used in Ref. 46 to study the water dynamical behaviors related to the onset, by cooling, of the LDL phase and accompanied by the underlying growth of the HB network structure.

the data (open symbols) corresponding to the cited MD simulation (TIP4P/2005 model)³¹ and confined water^{34,35} are also included. Just on looking only at the bulk water V_S data, it is evident that the general shape of the isobars follow similar trends as that of the ambient pressure with the drop between the low and high volume regions (typical of the LDA or where the LDL dominates) that becomes increasingly sharper as P increases. Although the behavior of these data as a function of T suggests a continuous evolution (as proposed by the MD and confined water data), by decreasing T from the HDL to the LDL and finally to the LDA, a full evaluation of κ_T (or α_P) cannot be obtained for the unexplored no man's land.

A help to overcome this problem comes from the careful analysis recently made in the study of the diffusion data for the ambient pressure. The experimental data, also including the ones obtained by means of the cited pulsed-laser heating techniques,²⁹ have been very recently analyzed under the assumption that, at high temperatures, they are characteristic of "pure" HDL, whereas in the deep supercooled regime, they are characteristic of "pure" LDL. In these terms, a continuity in the evolution of the studied transport function has been assumed.⁴⁶ Such an analysis has been made by using the following form for the relevant observable, $O(T)$:

$$O(T) = s(T)O_{LDL}(T) + (1 - s(T))O_{HDL}(T),$$

where $O_{LDL}(T)$ and $O_{HDL}(T)$ are the (temperature dependent) observables corresponding to "pure" LDL and HDL, respectively, and $s(T)$ is a Logistic Function (LF), which is used for growth mechanisms.⁴⁶ Such a study has been made for the liquid water self-diffusion data at ambient pressure in the $126 < T < 262$ K range.²⁹ We highlight that such a hypothesis well accounts how liquid water, on decreasing T , evolves from the disordered HDL to the tetrahedral LDL and then to the LDA. The quality of the obtained results suggests that such a procedure can be extended to the density data, directly related to the system structure. Hence, by using such a form

that reflects the growth of the HB network structure and the development of the LDL phase, we have fitted the specific volume data ($O(T) = V_S(T)$) obtained from the liquid water experimental densities shown in Fig. 2. The results for the different isobars from 0.1 to 200 MPa are reported as curves in Fig. 5 together with the measured data. The only assumption that we did is that for the LDL, $V_S = 1.081 \text{ g}^{-1} \text{ cm}^3$ at 180 K, as suggested by the data evolution. We are aware that lacking experimental data inside the no man's land, such a procedure can be considered a speculation. However, it can be noted that the density data of the MD simulations³¹ and confined water^{34,35} have (i) the same values (within the experimental error) of that of bulk water measured inside the accessible region and (ii) the similar trends of the obtained LFs (in the no-man's land). Therefore, we thought that, by means of such a working procedure, at least valid and useful suggestions could be obtained.

In such a way, providing also inside the no man's land reasonable volume data, we can calculate κ_T in the range $190 < T < 680$ K at different isobars from 0.1 to 400 MPa. The obtained results are proposed in Fig. 6, whereas it can be observed that the isothermal compressibility shows two separate maxima. One κ_T maximum is located as expected very near the water liquid-vapor critical point at about $P \approx 20$ MPa and $T \approx 647$ K, and the second one is well inside the supercooled regime in the interval $225 > T > 195$ K, and in particular, it is observable only for $0.1 < P < 200$ MPa (with its temperature that decreases by increasing the pressure). As it can be observed, the figure reports κ_T in a log scale in order to give in proper way the data details, being the difference between the two maxima of about an order of magnitude (~ 550 and $\sim 4100 \text{ } 10^{-6} \text{ bar}^{-1}$). In any case, it can be also observed that for all the reported pressures, κ_T has the minimum at T^* , with a value that decreases by increasing P . In the figure inset, κ_T is instead reported in a linear scale, and it is evident that it has the largest value at 180 MPa and 197.5 K. In summary, such a κ_T behavior inside the supercooled regime (where the heights of the maxima increase with pressure and their positions shift toward lower temperatures) is certainly

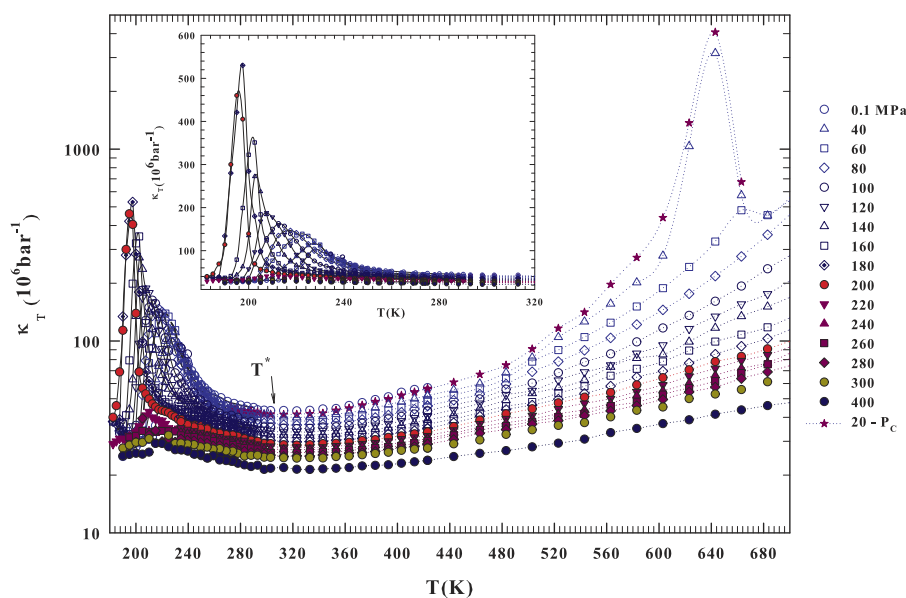


FIG. 6. The obtained κ_T isobars (range 0.1–400 MPa) in the range $190 < T < 680$ K. Two separate κ_T maxima are observable: one corresponding to the water liquid-vapor critical point ($P \simeq 20$ MPa and $T \simeq 647$ K) and the second one is well inside the supercooled regime. The data are reported in a log-lin scale in order to give a detailed representation, being the difference between the two maxima of about an order of magnitude (~ 550 and $\sim 4100 10^{-6}$ bar $^{-1}$).

the fingerprint of the approach to a critical point. The density and compressibility behaviors as a function of the pressure and temperature have also been studied by means of MD simulations, e.g., the mentioned TIP4P/2005,^{30,31} the E3B3^{32,52} and the iAmoeba⁵²

models, and a comparison of the κ_T^{\max} (near the LLCP) obtained in these studies and our present value of $\sim 550 10^{-6}$ bar $^{-1}$ reveals a satisfactory agreement especially with that evaluated by the iAmoeba model.

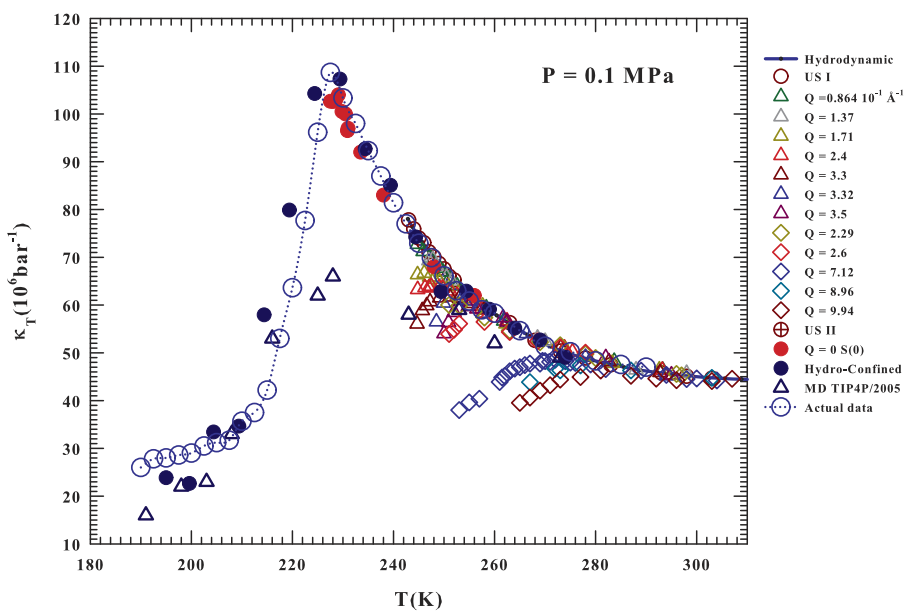


FIG. 7. The isothermal compressibility measured by elastic and dynamical scattering experiments (e.g., sound and hypersound propagation) as $\kappa_T(\omega, Q)$, and compared with its thermodynamical values. Dynamical data are based on the idea that the HB network is a relaxing structure and thus must be dependent of the probe frequency (ω) and wavevector (Q).⁴⁷ In such a way, $\kappa_T(\omega, Q)$, evaluated at ambient pressure, shows a maximum, κ_T^{\max} , that is, T and Q dependent: its value increases when these variables are decreased so that in the hydrodynamic regime, $Q \rightarrow 0$, it must correspond to the thermodynamical value. A situation confirmed by the figure where the actual and literature data are considered. In particular, Brillouin scattering^{48,49} and ultrasound data (US I⁵⁰ and US II⁵¹) are reported together with the recent data obtained by means of femtosecond x-ray experiments.⁵² κ_T data obtained with the cited MD (TIP4P/2005) study^{30,31,52} are also reported.

Before closing the discussion related to the proposed analyses of the density data, we have to mention that in the past, we have considered a study of the bulk water compressibility taking into account not only the hydrodynamic data but also the data coming from dynamical scattering (e.g., sound and hypersound propagation) on following the idea that at the basis of the LLT (and thus the LLCP), there is the presence of the “relaxing” HB network (or the LDL). Because such a structure grows inside the supercooled regime and is dynamical in character, it is a structure with precise relaxations that reasonably may be observed and emphasized by changing the radiation probe frequency (ω) or wavevector (Q).⁴⁷ In other words, we have evaluated $\kappa_T(\omega, Q)$ at the ambient pressure showing that its maximum κ_T^{\max} , observable also at the room temperature, is T and Q dependent and its value increases when these variables are decreased (see Fig. 7).^{48–51} With such an analysis, we have proposed, by using scaling concepts, that the bulk water compressibility hydrodynamic value ($\kappa_T(Q \rightarrow 0)$) has a maximum at $T_L = 228 \pm 5$ K, just where the α_P curves, obtained from the densities of confined water, have a minimum (at which, according to the thermodynamical relations among the response functions, must correspond a maximum in κ_T). Recently, such a maximum in the water compressibility has been shown by the Nilsson team in micrometer-sized water droplets by means of femtosecond x-ray experiments by a direct measure of the density structure function $S(Q) = (\rho/m)k_B T \kappa_T$, where m is the molecular mass⁵² (corresponding data are reported in Fig. 7). However, the findings of this latter study have been questioned: (i) for an inappropriate use of the Ornstein-Zernike formalism (*which is reliable near a critical point*), (ii) for the required knowledge of ρ , not available for $T < 239.74$ K,⁵³ and lately (iii) for the validity of the used temperature calibration scheme,⁵⁴ giving rise to a controversy.⁵⁵ It must be stressed that Nilsson *et al.*, together with this compressibility maximum,⁵² have also measured the density-density correlation length observing for such a function a maximum at 229 K, so providing a direct evidence of the Widom line in micrometer-sized water droplets (and thus in bulk), which is another support to the LLT. In the figure, the compressibility data obtained in the present study and those corresponding to the TIP4P/2005 MD study are also reported. As it can be observed, there is a good agreement, within the experimental error, with the x-ray data analysis for both the supercooled region experimental accessible data ($T < 239.74$ K) and those in the no man’s land. Instead, the agreement with the MD simulation study is only for the temperature value of the κ_T^{\max} .^{30,31,52}

III. CONCLUSION

In conclusion, we have to stress that our observations come only from the measured density data (Fig. 2) of bulk and amorphous water (LDA and HDA), as far as the only used conjecture. Just on looking at the different isobars from the ambient pressure (0.1 MPa) to 800 MPa as a function of the temperature (from the critical ~ 700 K to well inside the glass region ~ 100 K), one can observe a clear evidence from the data evolution of the presence, in the ρ - T phase diagram, of a phase region limited by two special values in the thermodynamic variables temperature and pressure, respectively, T^* and P^* : (i) T^* marks the onset of the HB transient tetrahedral network (and thus it is accompanied by a density-density correlation length larger than water intermolecular distance), and (ii) P^* is a crossover pressure between two well separated regions

in which the bulk water has the density maxima ($P < P^*$) or not ($P > P^*$). In addition, below such a special pressure and on cooling well inside the supercooled regime toward the glass, any bulk water isobar evolves only and only to the LDA, whereas for $P > P^*$, the only possible gelification is in the HDA glass. It can also be easily observed that the measured density of the LDA glass ranges in a narrow interval (0.9–0.93 g cm⁻³) and the HDA glass, observable only for $P > P^*$, has densities progressively larger than $\rho \approx 1.15$ g cm⁻³, as P increases. As evidenced by these behaviors at and around 135 K, the densities (or the specific volumes) in the range $0.93 < \rho < 1.15$ g cm⁻³ appear barred for glassy water. At the same time, as evidenced by the density isobars behaviors ($P > P^*$), there is no reason to believe that such a thermodynamical constraint is not valid near or below the homogeneous nucleation temperature T_h or also where the Widom line is located (e.g., the region 180–210 K).

Because liquid water is a mixture of LDL and HDL, as also fully supported by Fig. 2 data evolution, each density isobar behavior on cooling is due by the HDL continuous evolution toward the LDL by means of the growth of the HB network and finally in the LDA. This happens for pressures at which the LDL form is possible; otherwise, the HDL can evolve only to the HDA as fully demonstrated by the data behavior for $P > P^*$.

Being the LDL development governed by the HB network growth, in number and sizes, we have reasonably assumed, for each density (or volume) isobar, that such a process is governed by the same logistic function used in the description of the self-diffusion dynamical response functions⁴⁶ and that the LDL represents the largest part of the water liquid polymorphism at about 180 K, where it has about the same density of the LDA glass toward which the LDL evolves with continuity by decreasing T . Unfortunately, not having bulk water data inside the no man’s land, especially for $P < P^*$, it is possible to evaluate κ_T (and the LLCP presence) only at such a reasonable conjecture, strongly suggested by the data behavior and also by the available and accurate MD simulation results.^{30–32,52}

By following such an approach, we have evaluated the bulk water compressibility obtaining support for the presence in the supercooled regime of a LLCP at around 180 MPa and 197.5 K. The only problem is that if the κ_T maximum value is compared with that of the real water critical point at 647 K, a difference of about one order of magnitude is observable. On the basis of the illustrated findings, we planned a series of new accurate experiments on the bulk and amorphous water structure and dynamics in the T - P plane, just on looking also at the changes in the inter- and intramolecular water properties as far as to their correlations.

ACKNOWLEDGMENTS

The work at MIT was supported by the DOE Office of Basic Energy Sciences (BES) under the Award No. DE-FG02-90ER45429 since 1990 to May 2017.

REFERENCES

1. P. Ball, *Life’s Matrix: A Biography of Water*, 1st ed. (Farrar, Straus, and Giroux, New York, 2000), p. xvi, 417.
2. G. Galilei, “Intorno alle cose, che stanno in sù l’acqua, o che in quella si muovono,” in *Discorso al Serenissimo Don Cosimo II Gran Duca di Toscana* (Cosimo Giunti, Florence, 1612).

³L. Magalotti, "Esperienze intorno agli artificiali agghiacciamenti," in *Saggi di Naturali Esperienze Fatte Nell'Accademia del Cimento Sotto la Protezione del Serenissimo Principe Leopoldo di Toscana e Descritte dal Segretario di Essa Accademia* (Giuseppe Cocchini All'Insegna Della Stella, Florence, 1667), pp. 127–176.

⁴P. G. Debenedetti and H. E. Stanley, *Phys. Today* **56**(6), 40–46 (2003).

⁵R. J. Speedy and C. A. Angell, *J. Chem. Phys.* **65**, 851–858 (1976).

⁶P. H. Poole, F. Sciortino, U. Essmann, and H. E. Stanley, *Nature* **360**, 324–328 (1992).

⁷E. Rapoport, *J. Chem. Phys.* **46**, 2891 (1967).

⁸G. Nemethy and H. Scheraga, *J. Chem. Phys.* **36**, 3382 (1962).

⁹C. M. Davis and T. A. Litovitz, *J. Chem. Phys.* **42**, 2563 (1965).

¹⁰M. S. Jhon, J. Grosh, T. Ree, and H. Eyring, *J. Chem. Phys.* **44**, 1465 (1966).

¹¹B. Kamb, *Science* **150**, 205 (1966).

¹²J. C. Palmer, P. H. Poole, F. Sciortino, and P. G. Debenedetti, *Chem. Rev.* **118**, 9129–9151 (2018).

¹³F. X. Prielmeier, E. W. Lang, R. J. Speedy, and H.-D. Lüdemann, *Ber. Bunsengesellschaft Phys. Chem.* **92**, 1111–1117 (1988).

¹⁴S. Cerveny, F. Mallamace, J. Swenson, M. Vogel, and L. M. Xu, *Chem. Rev.* **116**, 7608–7625 (2016).

¹⁵J. H. Simpson and H. Y. Carr, *Phys. Rev.* **111**, 1201 (1958).

¹⁶F. Mallamace, C. Corsaro, D. Mallamace, C. Vasi, and H. E. Stanley, *Faraday Discuss.* **167**, 95 (2013).

¹⁷O. Mishima, L. D. Calvert, and E. Whalley, *Nature* **310**, 393–397 (1984); **314**, 76–78 (1985).

¹⁸O. Mishima, *Nature* **384**, 546–550 (1996).

¹⁹E. F. Burton and W. F. Oliver, *Proc. R. Soc. London, Ser. A* **153**, 166–172 (1935).

²⁰P. W. Bridgman, *Proc. Am. Acad. Arts Sci.* **47**, 441–558 (1912).

²¹T. Loerting, C. Salzmann, I. kohl, E. Mayer, and A. Hallbrucker, *Phys. Chem. Chem. Phys.* **3**, 5355 (2001).

²²K. Amann-Winkel, C. Gainaru, P. H. Handle, M. Seidl, N. Nelson, R. Bohmer, and T. Loerting, *Proc. Natl. Acad. Sci. U. S. A.* **110**, 17720–17725 (2013).

²³K. Amann-Winkel, R. Bohmer, F. Fujara, C. Gainaru, B. Geil, and T. Loerting, *Rev. Mod. Phys.* **88**, 011002 (2016).

²⁴P. H. Handle and T. Loerting, *J. Chem. Phys.* **148**, 124509 (2018).

²⁵P. Bruggeller and E. Mayer, *Nature* **288**, 569–573 (1980).

²⁶S. Sastry, P. G. Debenedetti, F. Sciortino, and H. E. Stanley, *Phys. Rev. E* **53**, 6144–6154 (1996).

²⁷A. K. Soper and M. A. Ricci, *Phys. Rev. Lett.* **84**, 2881–2884 (2000).

²⁸F. Mallamace, P. Baglioni, C. Corsaro, J. Spooren, H. E. Stanley, and S.-H. Chen, *Riv. Nuovo Cimento* **34**, 253 (2011).

²⁹Y. Xu, N. G. Petrik, R. Scott Smith, B. D. Kay, and G. A. Kimmel, *Proc. Natl. Acad. Sci. U. S. A.* **113**, 14921–14925 (2016).

³⁰J. L. Abascal and C. Vega, *J. Chem. Phys.* **133**, 234502 (2010).

³¹J. L. Abascal and C. Vega, *J. Chem. Phys.* **134**, 186101 (2011).

³²Y. Ni and J. L. Skinner, *J. Chem. Phys.* **144**, 214501 (2016).

³³J. A. Sellberg *et al.*, *Nature* **510**, 381–384 (2014).

³⁴F. Mallamace, C. Branca, M. Broccio, C. Corsaro, C.-Y. Mou, and S.-H. Chen, *Proc. Natl. Acad. Sci. U. S. A.* **104**, 18387–18391 (2007).

³⁵M. Erko, D. Wallacher, A. Hoell, T. Hauf, I. Zizak, and O. Paris, *Phys. Chem. Chem. Phys.* **14**, 3852–3858 (2012).

³⁶T. Grindley and J. E. Lind, *J. Chem. Phys.* **54**, 3983–3989 (1971).

³⁷G. S. Kell, *J. Chem. Eng. Data* **20**, 97–105 (1975).

³⁸G. S. Kell and E. Whalley, *J. Chem. Phys.* **62**, 3496–3503 (1975).

³⁹C. M. Sorensen, *J. Chem. Phys.* **79**, 1455–1461 (1983).

⁴⁰D. E. Hare and C. M. Sorensen, *J. Chem. Phys.* **84**, 5085–5089 (1986).

⁴¹D. E. Hare and C. M. Sorensen, *J. Chem. Phys.* **87**, 4840–4845 (1987).

⁴²O. Mishima, *J. Chem. Phys.* **133**, 144503 (2010).

⁴³A. Saul and W. Wagner, *J. Phys. Chem. Ref. Data* **18**, 1537 (1989).

⁴⁴F. Mallamace, C. Corsaro, and H. E. Stanley, *Sci. Rep.* **2**, 993 (2012).

⁴⁵J. Catalán and J. C. del Valle, *ACS Omega* **3**, 18930–18934 (2018).

⁴⁶N. J. Hestand and J. L. Skinner, *J. Chem. Phys.* **149**, 140901 (2018).

⁴⁷F. Mallamace, C. Corsaro, and H. E. Stanley, *Proc. Natl. Acad. Sci. U. S. A.* **110**, 4899–4904 (2013).

⁴⁸S. Magazú *et al.*, *J. Phys. Chem.* **93**, 942–948 (1989).

⁴⁹A. Cunsolo and M. Nardone, *J. Chem. Phys.* **105**, 3911–3917 (1996).

⁵⁰E. Trinh and R. E. Apfel, *J. Chem. Phys.* **72**, 6731–6735 (1980).

⁵¹A. Taschin, R. Cucini, P. Bartolini, and R. Torre, *Philos. Mag.* **91**, 1796–1800 (2011).

⁵²K. H. Kim, A. Späh, H. Pathak, F. Perakis, D. Mariedahl, K. Amann-Winkel, J. A. Sellberg, J. H. Lee, S. Kim, J. Park, K. H. Nam, T. Katayama, and A. Nilsson, *Science* **358**, 1589–1593 (2017).

⁵³F. Caupin, V. Holten, C. Qiu, E. Guillerm, M. Wilke, M. Frenz, J. Teixeira, and A. K. Soper, *Science* **360**, eaat1634 (2018).

⁵⁴C. Goy, M. A. C. Potenza, S. Dedera, M. Tomut, E. Guillerm, A. Kalinin, K.-O. Voss, A. Schottelius, N. Petridis, A. Prosvetov, G. Tejeda, J. M. Fernandez, C. Trautmann, F. Caupin, U. Glasmacher, and R. E. Grisenti, *Phys. Rev. Lett.* **120**, 015501 (2018).

⁵⁵K. H. Kim, A. Späh, H. Pathak, F. Perakis, D. Mariedahl, K. Amann-Winkel, J. A. Sellberg, J. H. Lee, S. Kim, J. Park, K. H. Nam, T. Katayama, and A. Nilsson, *Science* **360**, eaat1729 (2018).

⁵⁶R. E. Gagnon, H. Kiefte, M. J. Clouter, and E. Whalley, *J. Chem. Phys.* **92**, 1909 (1990).